

## WIRELESS INTRACRANIAL EEG DEVICE

### BACKGROUND

There are a number of shortcomings of the current methodology for intracranial EEG (icEEG) monitoring [1] including the need for an exit wound, tethering the patient to an external recording system, the need for a special environment for intracranial monitoring, and the limited scalability of the solution. The limitations of the present methodology increase morbidity, restrict mobility, limit monitoring to a specialized ward, restrict brain coverage, diminish the quality of observed signals and include cosmetic disfigurement which is not acceptable to some patients. These limitations could be considerably reduced by the wireless transmission of icEEGs from intracranial sensors to recording equipment external to the brain. We have developed a 64 channel wireless icEEG device for this purpose. The device was miniaturized to allow testing in the rat. We are adapting this solution to make a brain-implantable sensing and stimulating device (BISSD) to control seizures.

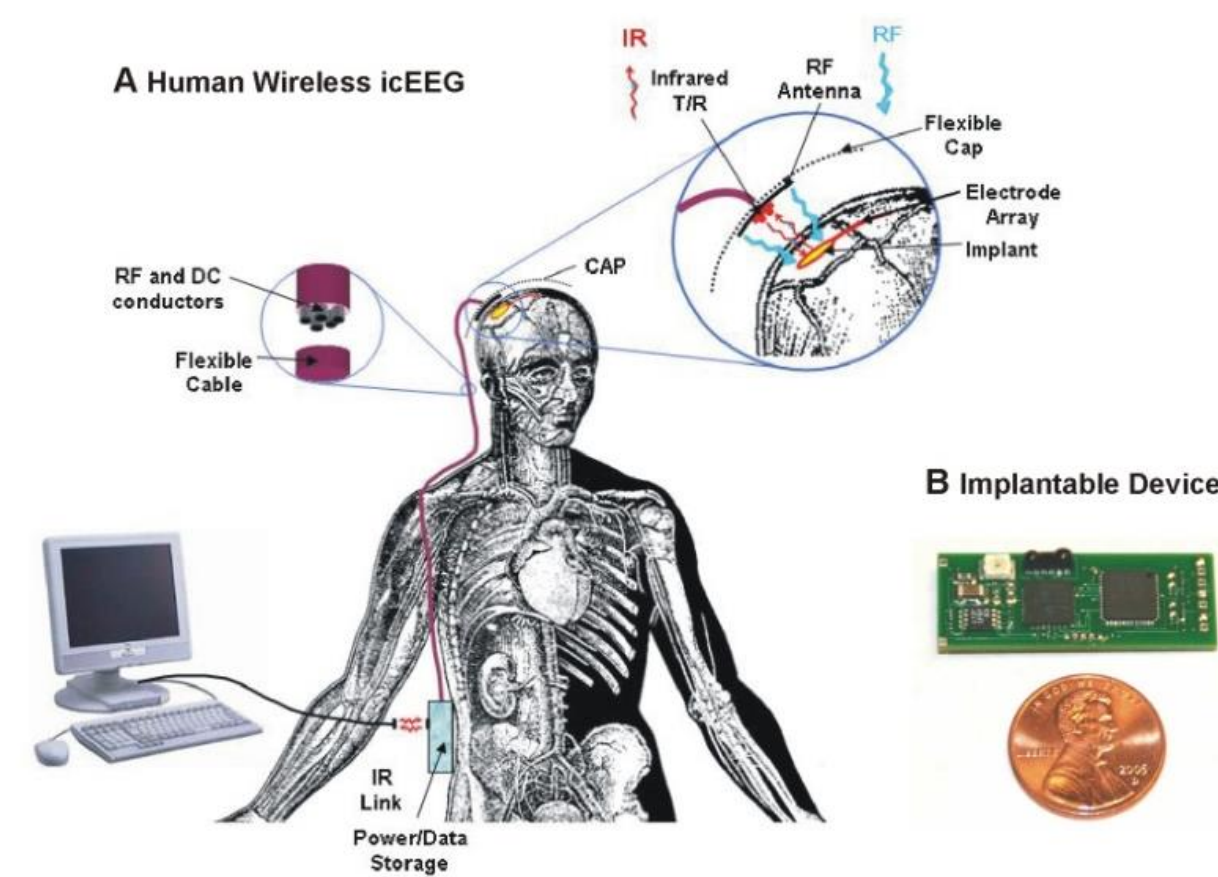


Figure 1. (a) Schematic of brain implantable 64 channel, battery-free, wireless digital icEEG acquisition system developed for human icEEG measurement. The device can condition, digitize and transmit digital icEEGs over an infrared link, be powered by RF, external wired power, or an integrated battery and used for animals or humans. (b) Implantable 64-channel icEEG recording device compared to a USA penny. The circuit board dimensions are 1.3 cm x 3.4 cm x 0.5 cm. The circuitry is built from current off-the-shelf (COTS) discrete technologies.

Test transmissions were performed in bench-top, ex-vivo and in-vivo evaluations of the 64-channel wireless icEEG device. The in-vivo test included transcutaneous icEEG transmission from a rat implanted with the wireless icEEG device.

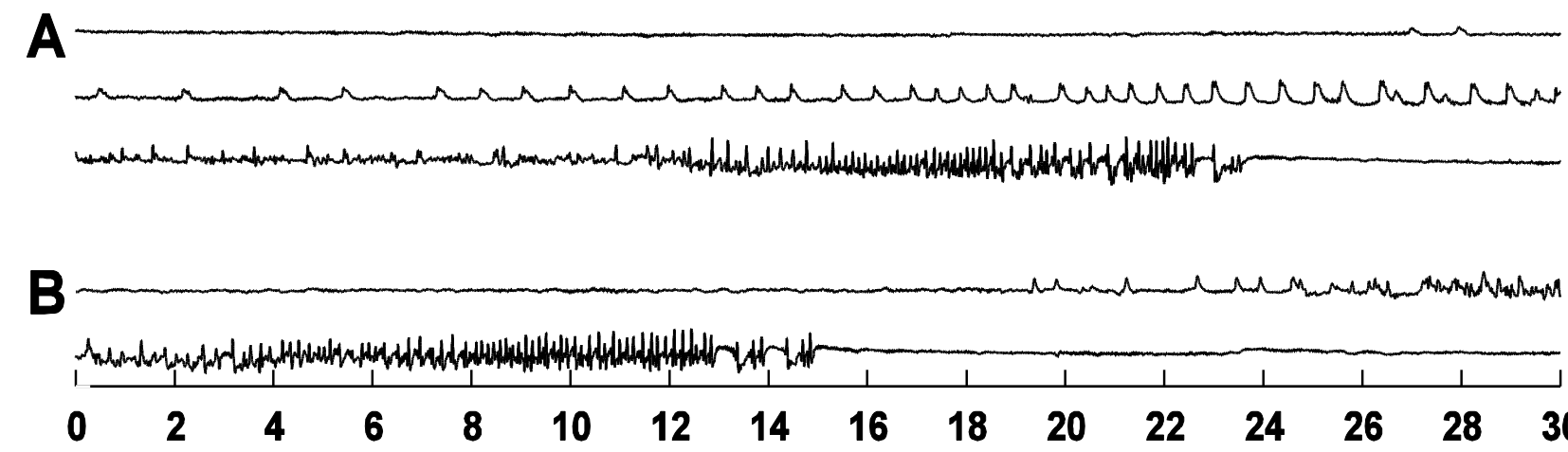


Figure 2. Two seizures which were recorded in a rat model of epilepsy with the 64 channel wireless device are displayed. Here, each trace is 30 sec in duration. (A) 90 sec continuous trace with an approximately 56 sec seizure. (B) 60 sec continuous trace with an approximately 25 sec seizure.

### SEIZURE DETECTION

We have tested multiple methods for detecting seizures such as those shown in Fig. 2. Our results indicate that we can detect seizures accurately within 5-6 seconds of onset. Additional work is underway to improve the time for detection to allow earlier detection. Earlier detection will allow greater control of seizures through closed loop feedback control using electrical stimulation or drug infusion.

### METHODS

We designed, fabricated and tested a prototype 64 channel brain implantable device for the wireless transmission of icEEGs (Figs. 1 and 2). The device, which was constructed from off-the-shelf electronic components, allows digital icEEG acquisition and transmission through a standard infra-red (IR) data link. The device can be powered by an embedded battery, wired external power or battery free power through a radio frequency (RF) power link. We are currently adapting this recording technology for continuous monitoring in a rat photo-thrombosis model for stroke and epilepsy (Fig. 3).

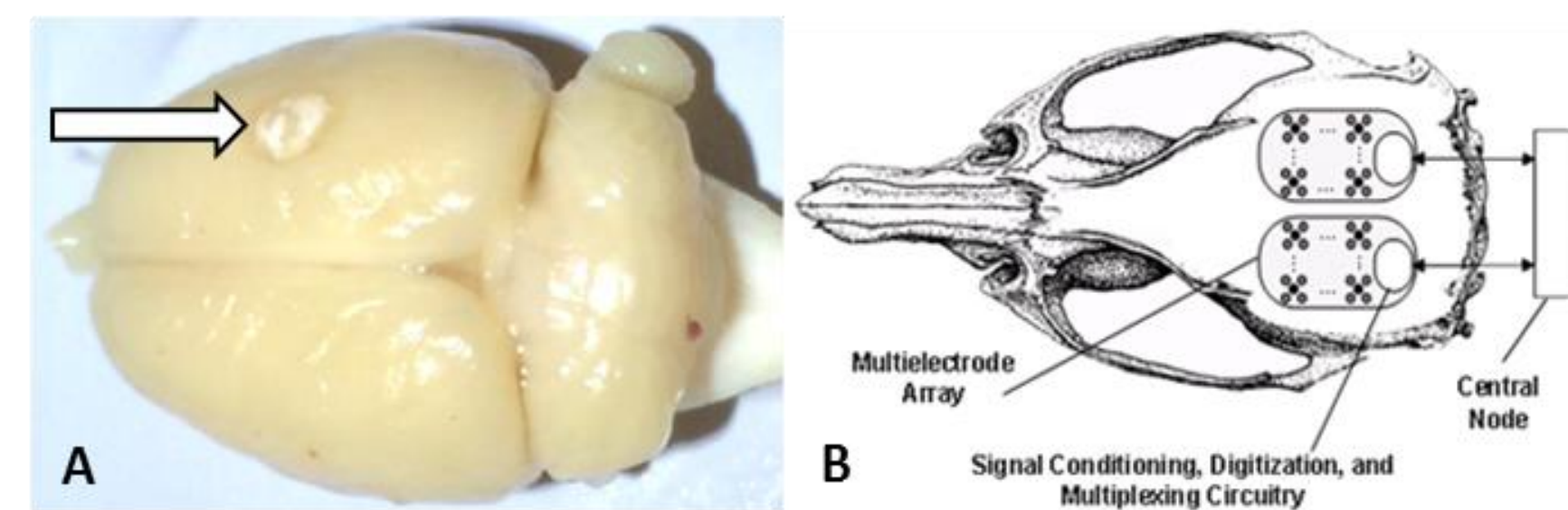


Figure 3. A. Stroke created on right hemisphere. B. Placement of the implantable system. There will be two thin-film grid electrodes, one per hemisphere, each with 8 x 4 primary contacts. The central node will be placed subcutaneously behind the shoulder.

### RESULTS

The brain activity in the rat will be recorded with a multi-contact grid electrode (Fig. 4). The electrode has multiple contacts so that it can sample the stroke infarct areas, areas on the periphery of the infarct, and areas relatively distant from the infarct (for comparison). A grid electrode is being designed for use in the rat. The design has been customized for the photo-thrombosis animal model.

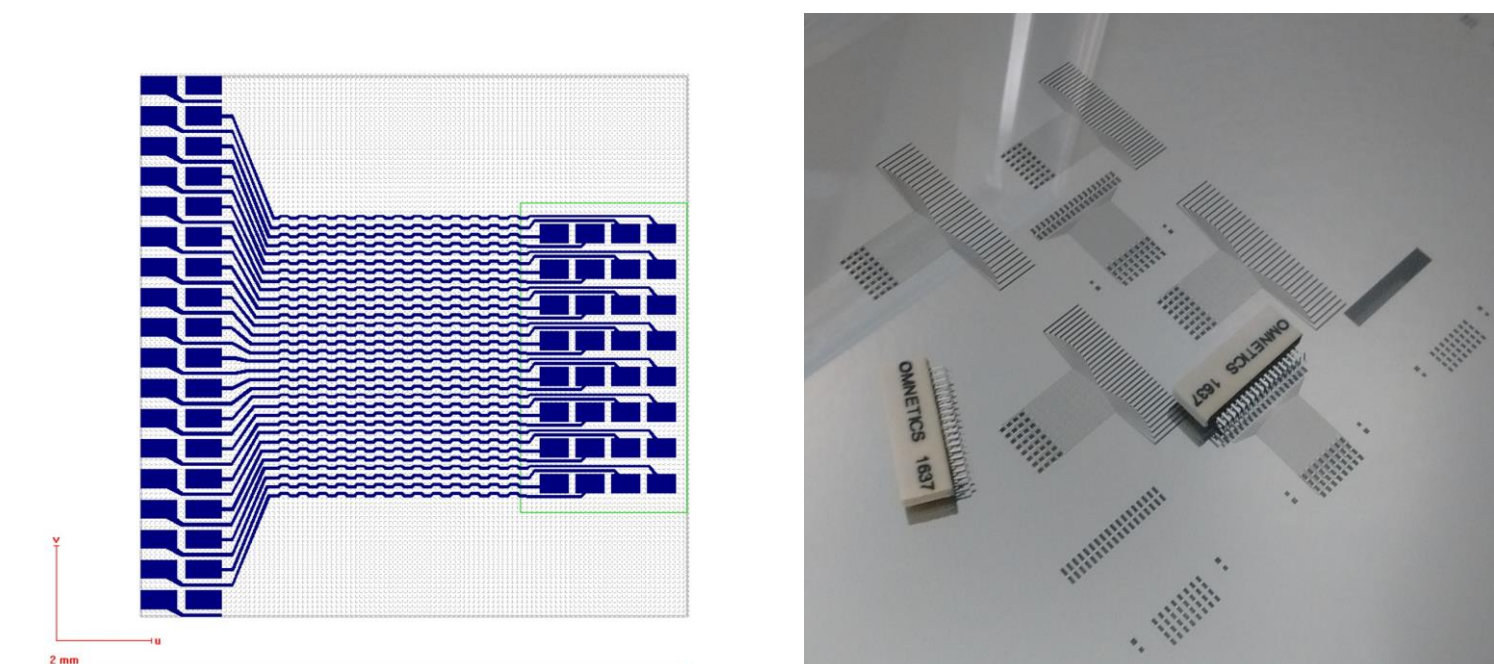


Figure 4. The layout (left) of a 32 channel intracranial grid electrode. The size of the 8 x 4 contact grid is 6 x 3 mm. Photomask (right) shown with an Omnetics connector. The grid will be connected to an icEEG acquisition system with an Omnetics connector.

### CONCLUSIONS

The preliminary tests conducted demonstrate proof-of-principle for an implantable solution to sense, condition, amplify, digitize and wirelessly transmit icEEGs. This technology has potential benefits for a BISSD.

## FAULT TOLERANT MULTIELECTRODE ARRAY

### BACKGROUND

An era of brain implantable devices has been ushered in recent years. Surprisingly, though, these vital devices do not incorporate fault-tolerance strategies which are de rigueur for other critical engineering devices. We present an argument for the inclusion of fault-tolerance in brain implantable devices to extend their dependability [2]. We focus, here, on multielectrode arrays (MEAs) for continuous monitoring of brain electrical activity.

### METHODS

We propose two redundancy based solutions to improve the dependability of MEAs. The first solution uses rows or columns of spare modules to replace faulty primary modules within a MEA. The second solution uses space redundancy with local reconfiguration in an interstitial redundancy array (IRA) form-factor. Here spare modules are placed in interstitial sites and can replace neighboring primary faulty modules. Different fault-tolerant solutions with varying redundancy ratio have been developed. The redundancy ratio is the ratio of the number of spare modules to the number of primary modules. A maximum matching graph algorithm is used to match faulty primary to available spare modules to reconfigure a faulty MEA. The IRA based design is described here (Fig. 5).

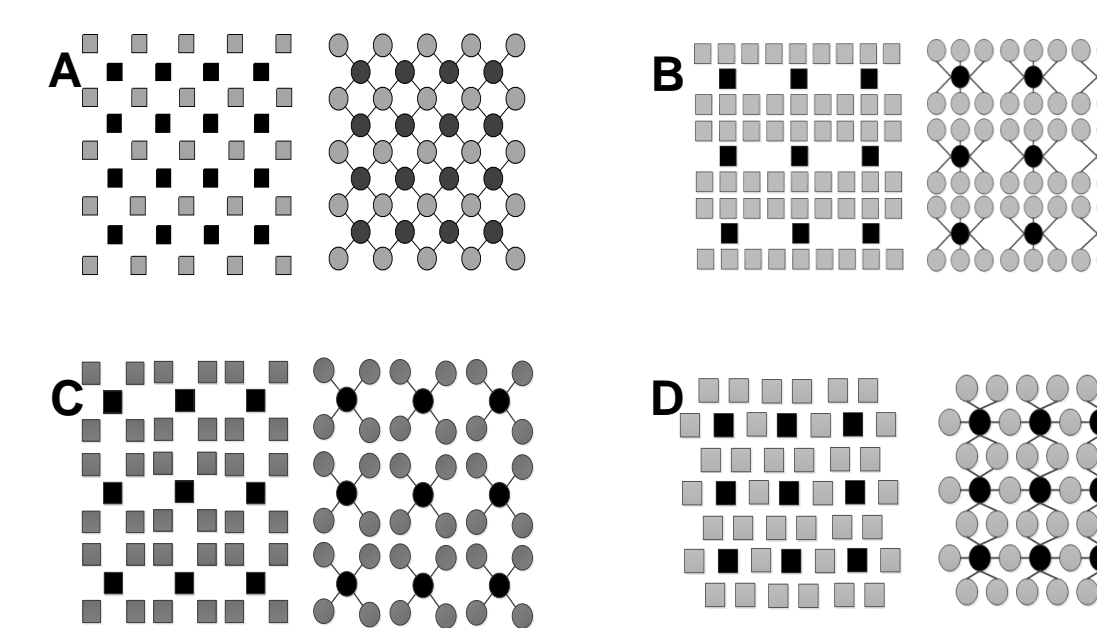


Figure 5. Example IRAs and their corresponding graph models are shown. In an IRA design spare modules (black) are located at the interstitial sites of the primary modules (gray). In an (s, p) IRA, each non-boundary primary module can be replaced by one of s spare modules and each non-boundary spare module can serve as a spare for p primary modules. Gray nodes in the graph represent primary modules and black nodes represent spare modules. If a spare module can replace a primary module, then there is an edge between the two nodes in the graph. (a) (4, 4) IRA, (b) (1, 6) IRA, (c) (1, 4) IRA, (d) (2, 6) IRA.

### RESULTS

We derived analytical expressions for the reliability of the different solutions and simulated the performance of these solutions under different fault conditions to characterize the dependability of a fault-tolerant MEA (Figs. 6 and 7).

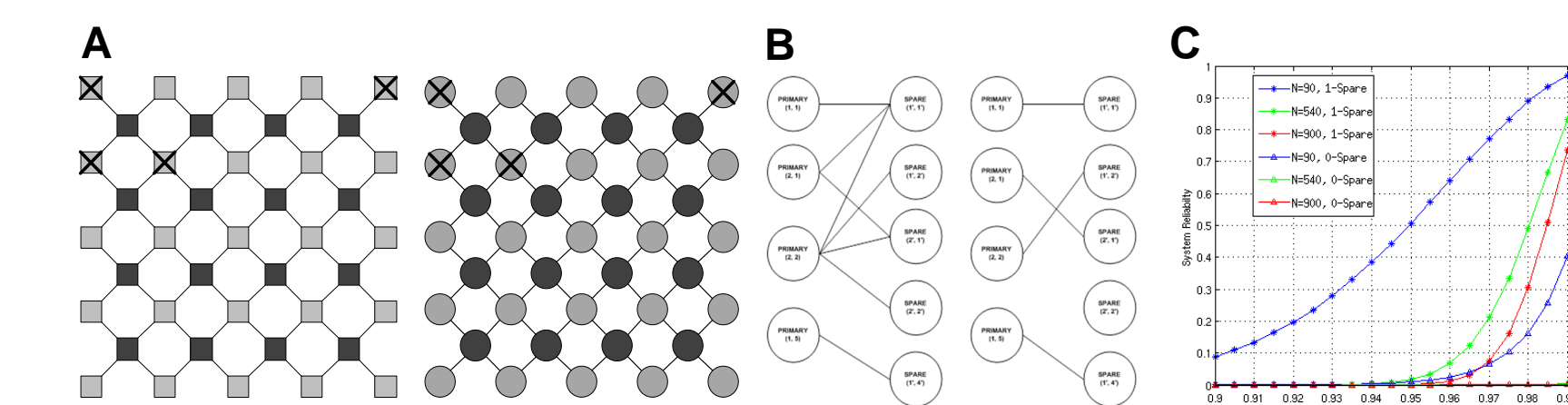


Figure 6. (a) A (4, 4) IRA with faults in 4 primary modules and the corresponding graph for this MEA. (b) The maximum matching solution to replace the faulty primary modules shown in (a). (c) An evaluation of MEA reliability as a function of module reliability for a (4, 4) IRA and a corresponding MEA without spare modules. Reliability is the probability that if the MEA is operational at a given point in time, it will remain operational at the next point in time. The evaluation of reliability was performed for MEAs where the number (N) of sensors was  $N = nm = 90, 540$  and  $900$  (where, n and m are the number of rows and columns of the MEA, respectively). There is a considerable increase in MEA reliability with the inclusion of spare sensors.

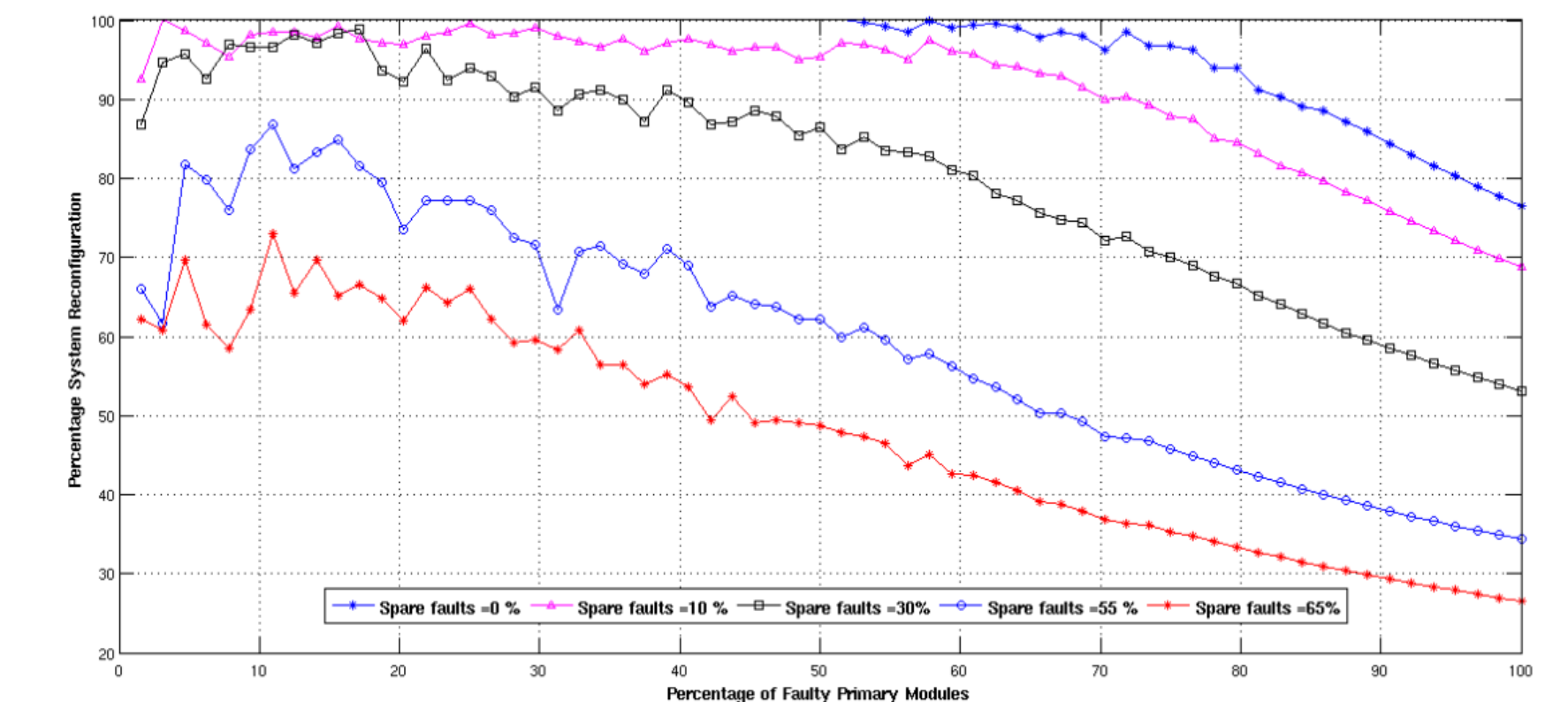


Figure 7. Simulation of fault reconfiguration for a (4, 4) IRA with MEA size  $N = 64$ ; with fault-coverage factor,  $C = 1$ ; and for different percent failed spares. Fault coverage, C, is a measure of an MEA's ability to recover from faults and continue to operate correctly. It is expressed as the probability that an MEA can recover from a fault, given a fault has occurred. In this simulation faults are injected at random locations in the MEA. The MEA was allowed to reconfigure itself using the maximum matching algorithm. The percentage of instances when the MEA could fully reconfigure itself is displayed as a function of percent primary faults, and percent spare faults.

### CONCLUSIONS

Redundancy increases cost and development time and may impact power consumption, heat generation, mass, and volume of an implantable device. A fault-tolerant design thus requires a trade-off between dependability and the amount of redundancy required to achieve it. The results of our analysis demonstrate that a considerable improvement in MEA dependability can be achieved with a well-designed increase in redundancy.

### REFERENCES AND PATENTS

#### REFERENCES

- Lanning B, Joshi BS, Kyriakides TR, Spencer DD, Zaveri HP, Emerging technologies for brain implantable devices, *Epilepsy: The Intersection of Neurosciences, Biology, Mathematics, Engineering and Physics*, Editors: Osorio I, Zaveri HP, Frei MG, Arthurs S, CRC Press, 2011.
- Acharya I, Joshi B, Lanning B, Zaveri HP, Reconfigurable fault-tolerant multielectrode array for dependable monitoring of the human brain, *Conference Proceedings IEEE Eng Med Biol Soc*, 652-5, 2011.
- M. A. Sayeed, S. P. Mohanty, E. Kougianos, and HP Zaveri, "eSeiz: An Edge-Device for Accurate Seizure Detection for Smart Healthcare", *IEEE Transactions on Consumer Electronics (TCE)*, Volume 65, Issue 3, August 2019, pp. 379--387.
- M. A. Sayeed, S. P. Mohanty, E. Kougianos, and HP Zaveri, "Neuro-Detect: A Machine Learning Based Fast and Accurate Seizure Detection System in the IoMT", *IEEE Transactions on Consumer Electronics (TCE)*, Volume 65, Issue 3, August 2019, pp. 359--368.

#### PATENTS

- Wireless system for epilepsy monitoring and measurement. DA Putz, BS Joshi, B Lanning, JA Nolan, GJ Nuebel, DD Spencer, HP Zaveri. Approved 2012.
- Wireless system for epilepsy monitoring and measurement. B Lanning, JA Nolan, GJ Nuebel, DD Spencer, HP Zaveri, Continuation in Part, Approved 2014.
- Wireless system for epilepsy monitoring and measurement. B Lanning, JA Nolan, GJ Nuebel, DD Spencer, HP Zaveri, Continuation in Part, Approved 2016.
- Fault-tolerant multielectrode array for brain implantable device. BS Joshi, I Acharya, HP Zaveri. Approved 2016.